

Specific Alteration of Spontaneous GABAergic Inhibition in Cerebellar Purkinje Cells in Mice Lacking the Potassium Channel Kv1.1

Chuan-Li Zhang,¹ Albee Messing,² and Shing Yan Chiu¹

¹Department of Physiology, University of Wisconsin School of Medicine, Madison, Wisconsin 53706, and ²Department of Pathobiological Sciences, School of Veterinary Medicine, and Waisman Center, University of Wisconsin, Madison, Wisconsin 53705

In the cerebellum, the basket cell innervation on Purkinje cells provides a major GABAergic inhibitory control of the single efferent output from the cerebellum. The Shaker-type K channel Kv1.1 is localized at the axon arborization preceding the terminal of the basket cells and is therefore a potential candidate for regulating the GABAergic inhibition. In this study, we directly assess this role of Kv1.1 by electrophysiological analysis of Kv1.1 null mutant mice. Whole-cell patch-clamp recordings of spontaneous IPSCs (sIPSCs) were made from Purkinje cells in thin cerebellar slices from postnatal day (P)10–15 Kv1.1-null mutants using wild-type littermates as controls. The null mutation confers a very specific change in the sIPSC: the frequency increases about twofold, without accompanying changes in the mean and variance of its amplitude distribution. The frequency and amplitude of the miniature IPSCs (mIPSCs) are unaffected.

Spontaneous firing rate of the basket cells is unaltered. Evoked IPSC does not show multiple activity in the mutants. Motor skills tests show that Kv1.1 null mice display a compromised ability to maintain balance on a thin stationary rod. We conclude that the Kv1.1 null mutation results in a persistent elevation of the tonic inhibitory tone on the cerebellum Purkinje cell efferent and that this is not fully compensated for by residual Shaker-type channels. We further suggest that the increase in inhibitory tone in the mutants might underlie the behavioral deficits. At the cellular level, we propose that Kv1.1 deletion enhances excitability of the basket cells by selectively enhancing the likelihood of action potential propagation past axonal branch points.

Key words: potassium channel gene; homologous recombination; cerebellum; GABA; mouse; Purkinje cell

The cerebellum is thought to be an important integration site in the CNS for motor coordination and certain types of learned motor behavior (Eccles et al., 1967; Kim and Thompson, 1997). The Purkinje cell provides the single efferent output from the cerebellum and is strongly modulated by a GABAergic inhibition strategically located at the initial segment that constitutes the last functional site for signal modulation before the efferent emerges from the cerebellum.

What is the molecular determinant of this GABAergic inhibition? In the cerebellum, two members of the Shaker potassium channel family (Kv1.1 and Kv1.2), as well as two auxiliary subunits (Kv β 1 and Kv β 2), are highly expressed in the basket cell arborization, or “pinneau,” that embraces the Purkinje cell initial segments (McNamara et al., 1993; Wang et al., 1994; Rhodes et al., 1995, 1996; Veh et al., 1995; Laube et al., 1996; McNamara et al., 1996). High-resolution electron microscopic analysis of Kv1.1 and Kv1.2 immunoreactivity reveals that these K channel subtypes are uniquely localized at septate-like junctions adjoining basket cell axons that precede the terminal (Wang et al., 1994). These Shaker K channels might therefore be candidates for regulating GABA release. However, their unique localization at axon arborizations

that precede the nerve terminal raises two questions: first, do they in fact regulate GABA release, and second, does the regulation involve novel mechanisms? The unique morphological feature of the pinneau has led to suggestions that inhibition at this site might be nonconventional and partly electrical in nature, involving excitability modulation by current flows in unusual resistance regions created by the septate-like junctions (Korn and Faber, 1980).

Proper modulation of the GABAergic inhibition at the pinneau of the cerebellum might be important for motor functions. Mutations of Kv1.1 in humans result in “episodic ataxia,” a disorder characterized by stress-inducible hyperexcitability of the nervous system (Browne et al., 1994). The role of cerebellar dysfunction in this disease is unclear, and it remains possible that the ataxia may reflect, in part, abnormal GABAergic inhibition consequential to Kv1.1 mutation, resulting in a shift in the balance between excitatory and inhibitory signal integration in the cerebellum.

Recently, analysis of the functional role of Kv1.1 in normal cellular physiology has been made possible by the generation of Kv1.1 null mutant mice through homologous recombination in embryonic stem cells (Smart et al., 1998). Various neurological defects were found. In the CNS, these mice exhibit spontaneous seizure activities with elevated excitability in hippocampal brain slices (Smart et al., 1998). In the peripheral nervous system, the excitability of the transition zone near the nerve terminal becomes abnormally temperature sensitive (Zhou et al., 1998). Furthermore, motor dysfunction unrelated to seizures was revealed when the Kv1.1 null mutants were forced to swim in cold

Received Nov. 18, 1998; revised Jan. 26, 1999; accepted Jan. 27, 1999.

This work was supported by Grant RO1-23375 from National Institutes of Health to S.Y.C. and A.M. We thank Tammy Robbins and Denise Springman for expert technical assistance.

Correspondence should be addressed to S.Y. Chiu, Department of Physiology, University of Wisconsin School of Medicine, 1300 University Avenue, 285 Medical Science Building, Madison, WI 53706.

Copyright © 1999 Society for Neuroscience 0270-6474/99/192852-13\$05.00/0

water and included neuromyotonia and inability to maintain an axial position while swimming (Zhou et al., 1998).

In this paper, we examined cerebellar physiology in the Kv1.1 null mice by a direct measurement of the GABAergic inhibition in cerebellar slice recordings and by behavioral tests. Our results reveal a specific action of Kv1.1 on basket cell excitability, as well as a subtle defect in balancing skill. We hypothesize that in basket cells, Kv1.1 regulates GABA release by regulating action potential failures at axonal arbors preceding the nerve terminal, thereby determining the fraction or the timing of action potentials reaching the nerve terminal.

MATERIALS AND METHODS

Kv1.1 null mice

The Kv1.1 mutant mice used in this study were generated by Smart et al. (1998) and maintained in a mixed B6x129 genetic background by heterozygote-heterozygote mating. They were genotyped as described previously (Zhou et al., 1998). Briefly, the mice were genotyped at postnatal day 7 (P7) using a PCR strategy on DNA prepared from tail biopsies, and experiments were done at P10–P15. Controls consisted of age-matched littermates that were +/+ at the Kv1.1 locus.

Electrophysiology

Cerebellar slices. Sagittal slices of cerebellum (150–200 μm) were prepared from P10–P15 mice. Briefly, the head was placed in ice-cold Ringer's solution after decapitation. The whole cerebellum was quickly removed and glued to the bottom of a dish with Superglue for slicing using a Vibratome (Series 1000, TPI). Slicing was performed with the cerebellum fully submerged in ice-cold Ringer's solution bubbled with 5% CO_2 + 95% O_2 . The slices (up to 6–10 from each animal) were transferred to a chamber at 37°C in which the solutions were continuously gently stirred by bubbling with 5% CO_2 + 95% O_2 . The slices were incubated in this chamber for at least 1 hr before they were transferred to a recording chamber for patch-clamp experiments. We waited 20–30 min after the transfer from 37°C to room temperature before the recordings were started.

Purkinje cell recordings. Whole-cell voltage-clamp recordings of spontaneous postsynaptic currents were made from visually identified Purkinje cell somas with an EPC-7 amplifier. Series resistance was compensated according to the procedure described by Llano et al. (1991). Briefly, after whole-cell formation, the slow transient cancellation and the G-series adjustment of the EPC-7 amplifier were adjusted to compensate the initial portion of the capacitance transient elicited by 10 mV hyperpolarizing pulses. The series resistance compensation knob of the EPC-7 amplifier was then set at 35–50%. Electrodes were pulled from borosilicate glass capillaries (1B120F-4, World Precision Instruments) and fire-polished to yield a resistance of 3–4 M Ω before seal formation.

Basket cell recordings. Cell-attached recordings were made from the soma of interneurons located in the innermost one-third of the molecular layer within a distance of 40 μm from the Purkinje cell body layer, as described previously (Vincent and Marty, 1996). Following Ramon y Cajal's (1911) classification, these interneurons were considered to be basket cells (Llano et al., 1997). We were primarily interested in the action potential frequency in the basket cells. In the cell-attached mode, action potentials at the soma generate action currents, detected with the holding potential at the pipette set at 0 mV, as described previously (Vincent and Marty, 1996). Basket cell bodies can be easily distinguished from the much smaller granule cells. The few recordings that did not give action potentials were discarded and were assumed to be from Bergmann glial cells.

Evoked IPSCs. Evoked IPSCs in Purkinje cells were elicited by extracellular stimulation of the inner one-third of the molecular layer using a double-barreled glass pipette pulled to a fine tip. The distance between the Purkinje cell under recording and the stimulation pipette was \sim 200 μm , measured horizontally along the inner molecular layer. A Grass Stimulator (S48) was used to deliver stimulating pulses with amplitudes ranging from 10 to 100 V. The duration of the pulse was 0.3 msec, and stimulation frequency was 0.5 Hz.

Data analysis

Current integral. We use an integration method as a convenient and unbiased means to compare wild-type and mutant spontaneous current

records. We integrated the spontaneous current records over a fixed short segment (1.23 sec) and performed this integration every 0.3 sec along continuous current records.

Event analysis. Each experiment consisted of 10–60 min continuous recording of spontaneous postsynaptic currents at a holding potential of -60 mV. During the experiment, the spontaneous currents were recorded continuously onto VCR tapes without filtering (highest bandwidth). After an experiment, the tapes were played back, and the currents were redigitized (Digidata 2000, Axon Instruments) at 2 kHz after being filtered at 1 kHz by an eight-pole Bessel filter (Frequency Device). The digitized data were analyzed either with pClamp 6.0 software (Axon Instruments) or with the event analysis software CDR (Computer Disk Recorder, J. Dempster, University of Strathclyde, Glasgow, UK). Event analysis was typically performed on continuous segments of spontaneous current records lasting 3–5 min. Histograms were made of two parameters extracted from the continuous records: the amplitude and the inter-event time interval. The amplitude of an event is defined as the difference between a short baseline segment (typically 0.1 msec) just before the rapid current increase and the peak of the current. The inter-event interval is defined as the time between the onset of the current rise of consecutive events. These two parameters were extracted from continuous current records using the CDR software in a semi-automatic manner.

To avoid biasing data analysis of the mutant and wild-type slices, all whole-cell experiments were recorded at the same gain of 2 mV/pA, and the threshold for event detection was fixed at 5 pA for all the results reported in this paper. Furthermore, "blinded" experiments were performed in which the genotype of the slice under study was known only by an independent observer and revealed only at the end of the event analysis. Of the 27 mice used for each genotype in Figures 1C and 3A,B, blinded experiments were performed on 15 mice in each group. In terms of individual cells, 30 of a total of 53 cells in those figures were obtained from blinded experiments. All data were expressed as the mean \pm SEM, with *p* values calculated using either independent or paired *t* tests from the software Origin (Microsoft).

Solutions and drugs. Experiments were performed at room temperature (22–24°C) using an extracellular bath solution composed of (in mM): NaCl 125, KCl 3, NaHCO_3 26, MgCl_2 1.0, CaCl_2 2, NaH_2PO_4 1.25, and glucose 10. Drugs were added to this solution as needed. Excitatory amino acid-mediated transmission was blocked by adding APV (100 μM) and CNQX (10 μM ; RBI). K channel blockers (α -dendrotoxin and I-dendrotoxin) were obtained from RBI. The solution was maintained during an experiment at pH 7.4 by bubbling with 5% CO_2 + 95% O_2 . The slice in the recording chamber was continuously perfused at a rate of 5 ml/min. The patch-clamp pipette for whole-cell Purkinje cell recording was filled with a solution containing (in mM): CsCl 140, EGTA 1, Na-ATP 4, Na-GTP 0.4, MgCl_2 4.6, CaCl_2 0.1, and HEPES 10, to pH 7.3 with CsOH. In some experiments, QX-314 (2 mM; RBI) was added to the pipette solution to block Na channels intracellularly to inhibit regenerative action potentials coming from parts of the cell (such as dendrites) that may not be under space clamp. For cell-attached recordings from basket cells, the pipette solution contained (in mM): NaCl 150, KCl 2.8, CaCl_2 1.0, and HEPES 10, pH 7.3.

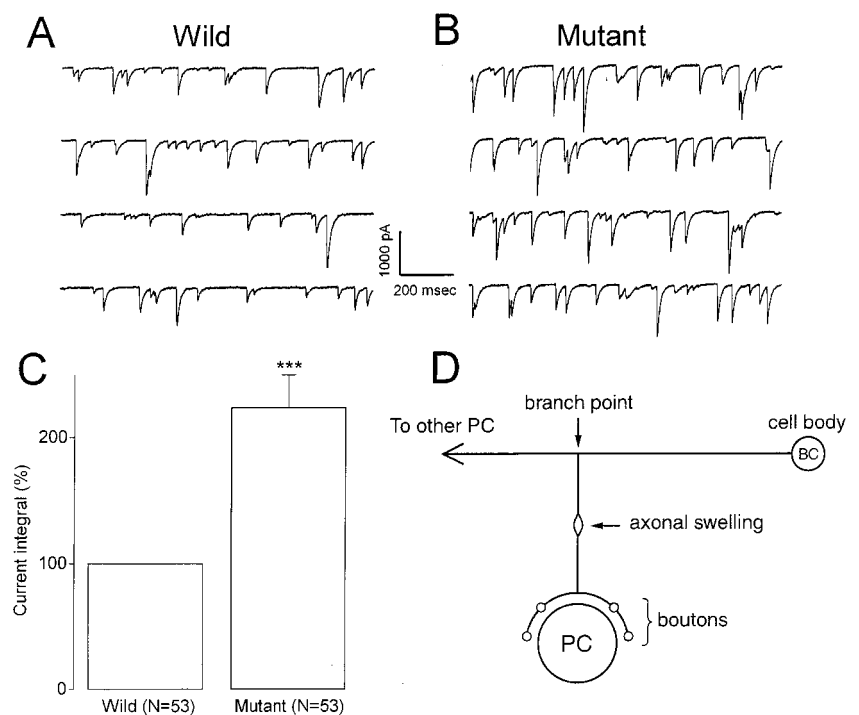
Electroencephalography

Electroencephalographs (EEGs) were recorded from mice as described previously (Zhou et al., 1998). Briefly, two EEG recording electrodes were implanted surgically in the left hemisphere of anesthetized mice. The electrodes made contact only, but did not pierce the cortex, and were fixed to the cranium with dental acrylic. The two leads from the electrodes were fed into the positive and negative inputs of a differential amplifier (World Precision Instruments). EEG recordings were made to exclude the presence of epilepsy during a motor skill test, as described below.

Motor skills tests

Stationary thin rod. Mice were placed in the middle of a thin rod, and the time they stayed on the rod before falling off (retention time) was measured. The rod was 15 mm in diameter and 50 cm long and placed 40 cm high to discourage jumping. The rod was flanked at both ends by a large smooth surface to prevent falling off at the end of the rod. The whole test system was enclosed in a white opaque Plexiglas case to minimize outside distractions. When placed on the rod for the first time, mice tend to cautiously walk along the rod in one direction, and on reaching the end of the rod, they make a turn and explore the other direction. Most falls occur when the animal makes the turn. Tests were

Figure 1. Kv1.1 null mutation increases the current integral of the spontaneous postsynaptic currents in Purkinje cells. *A* shows four representative traces of spontaneous postsynaptic currents measured from a Purkinje cell of a P11 wild-type mouse. *B* shows a recording from an age-matched Kv1.1 null littermate. Holding potential was -60 mV at *A* and *B*. *C* compares the current integral of the postsynaptic currents in the wild type and the null. The postsynaptic currents were integrated over fixed 1.23 sec segments, and this current integral was computed every 0.3 sec along a 3 min continuous recording of postsynaptic currents. The current integrals were then averaged, and the mutant data were displayed as a percentage of the wild-type data. The current integral of the spontaneous current in the mutant was significantly different from that of the wild type [$224 \pm 26\%$ ($n = 53$) mutant; $100 \pm 12\%$ ($n = 53$); $p < 0.001$]. The experiments were performed at room temperature for the data in this and in all other figures. *D*, Hypothesis on the role of Kv1.1 in basket cell excitability. We propose that Kv1.1 deletion selectively improves the likelihood of action potential propagation across axonal branch points or axonal swellings, without affecting the excitability of the boutons and the cell body. *PC*, Purkinje cell; *BC*, basket cell. In this model, an action potential travels down the main axon, branches into a descending collateral, encounters an axonal swelling, and then invades four boutons embracing the Purkinje cell. Because the mean and variance of the amplitude distribution of the sIPSC (the successful events; Fig. 3*B*) are not affected by the mutation, we assume that the same number of boutons is being invaded for each successful action potential. The unreliability is therefore likely in propagating past the collateral branch point or the axonal swelling preceding the nerve terminal. The data in our paper can be explained if Kv1.1 deletion reduces the rate of conduction failure at either the collateral branch point or the axonal swelling. This scheme is based on the morphology of a biocytin-filled 13-d-old basket cell from the rat (Llano et al., 1997, their Fig. 5). Our hypothesis requires that Kv1.1 be expressed at or near the branch points, a requirement that is consistent with the unique staining of Kv1.1 at septate-like junctions in the axonal arborizations of basket cells described at the EM level (Wang et al., 1994).



repeated every day. After repeated trials, mice learned to stay on longer by not walking, or they became more skillful at the turns. Each mouse was first weighed before testing so that we could assess whether body weight was a factor that affected the retention time on the rod. For some mice, EEG recordings were made to determine whether the falls correlated with seizures. The mouse was first observed for 5 min and scored for signs of epilepsy both visually and through the EEG recordings. Then the mouse was placed on the stationary rod, and the retention time was measured, with EEG recordings made up to the time of fall. *Rotarod*. Mice were placed on a rotarod apparatus (50 mm diameter; Columbus Instrument). The speed of rotation was ramped from 4 to 40 rpm in 5 min and then allowed to stay at 40 rpm afterward. Four mice were tested at the same time, and partitions were placed to blocking them from seeing one another during the test. The retention time was measured. As in the stationary thin rod tests, the tests were repeated every day.

RESULTS

The primary goal of this study was to determine whether spontaneous GABAergic inhibition of Purkinje cells in the cerebellum is altered in the absence of Kv1.1 and to elucidate a possible mechanism for the alteration. Because spontaneous postsynaptic current activities show quite a large variation even among mice of the same genotype, we adopted several measures to avoid biasing the analysis. First, age-matched mutant and wild-type mice from the same litter were always used. Typically, recordings were performed on one mouse on 1 d followed the next day by a littermate of the opposite genotype. The order of the genotype was randomized to average out the 1 d difference in age of the two groups. Second, some of the experiments were blinded, and the genotype of the slice under study was revealed by an independent observer only after histograms were generated. Third, all currents were collected at the same gain, and the event analysis was performed with a fixed threshold for all slices regardless of genotypes. In all, the conclusion in this paper is based strictly on

this protocol applied to a total of 45 mutant mice with an equal number of age-matched, wild-type controls over an age range of P10–P15.

Kv1.1 null mutation increases the current integral of the spontaneous postsynaptic current

When a Purkinje cell soma in the cerebellum was subjected to whole-cell voltage clamp at a holding potential of -60 mV with a Cs-filled pipette and normal saline solution outside, spontaneous postsynaptic currents were observed. Figure 1 shows spontaneous postsynaptic currents recorded from the Purkinje cell of a wild-type (*A*) and a Kv1.1-null (*B*) slice. The mutant currents appeared to be more robust than the wild-type. The goal of this study was to document quantitative differences in the spontaneous currents between wild-type and Kv1.1 null. However, given the variation in these records, we felt that it was important, before pursuing quantitative analysis, to have a completely objective method of establishing whether the mutant currents were in fact different from the wild-type currents. We chose a convenient method that is based on the current integral, which is simply the charge. We took 3 min segments of continuous records from the wild-type and null slices and integrated the currents over 1.23 sec segments spaced uniformly over the entire 3 min segment (Fig. 1). The current integral of the 1.23 sec segments was averaged for the wild type ($n = 53$ cells) and mutant ($n = 53$ cells) and is shown in Figure 1*C*. This method demonstrates a clear increase of the current integral of the spontaneous postsynaptic currents in the mutant over the wild type in a manner that is completely independent of series resistance compensation, how the currents were filtered, or the electrical noise of the recording system. Having concluded that Kv1.1 indeed results in an enhancement of the

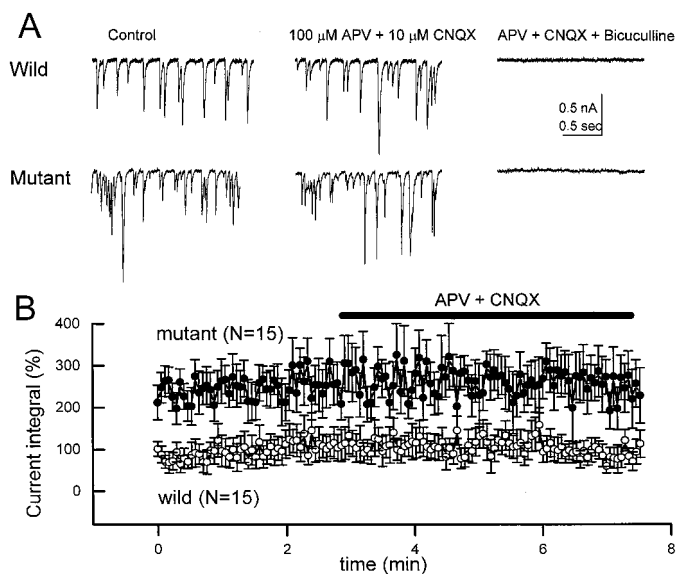


Figure 2. Excitatory transmission blockers have no effect on the spontaneous postsynaptic currents. *A* shows the sequential effect of 100 μ M APV + 10 μ M CNQX and APV + CNQX + 10 μ M bicuculline on the spontaneous postsynaptic currents in a null and a wild-type Purkinje cell. *B* shows the averaged result for the wild-type and the null mutant. The data points were generated by integrating 1.23 sec segments of spontaneous currents every 2.27 sec along the continuous recordings before and during drug application. Whole-cell recordings of spontaneous postsynaptic currents from Purkinje cells. Holding potential -60 mV.

spontaneous currents, we next proceeded to perform more elaborate event analysis to determine the quantitative aspects of the changes in the currents in the mutant.

The increase in spontaneous postsynaptic currents in the mutant is caused entirely by an increase in GABAergic inhibitory transmission

What is the nature of the spontaneous postsynaptic currents? The currents were measured at a holding potential of -60 mV, with approximately equal chloride concentration inside and outside of the cell. The sodium concentration was high outside and low inside. Under these conditions, inhibitory transmitters (opening chloride channels) and excitatory transmitters (opening cation permeable channels) will both generate a flow of equivalent positive charges into the cell, resulting in currents of the same direction flow (inward) as detected by the patch-clamp amplifier. In the case of wild-type Purkinje cells, Konnerth et al. (1990) have already demonstrated that the spontaneous currents recorded under these conditions are virtually all inhibitory and GABAergic in nature. We confirmed this observation in our wild-type slices. The addition of APV and CNQX, blockers of excitatory transmission, did not affect the spontaneous postsynaptic currents (Fig. 2*A,B*). When bicuculline was applied, all of the spontaneous activities were blocked (Fig. 2*A*). This confirmed that in the wild-type slice, the spontaneous postsynaptic currents are inhibitory in nature, attributable presumably to spontaneous release of GABA from basket cells.

How does the Kv1.1 mutation augment the spontaneous postsynaptic currents in the Purkinje cell? One mechanism is an increase in excitatory transmission. For example, the Kv1.1 mutation could recruit new excitatory synapses to directly innervate the Purkinje cell, or it could cause an increase of excitatory drive to the basket cells that normally produce the spontaneous

GABAergic activities on the Purkinje cell. This increase in spontaneous excitatory transmission, both monosynaptically and polysynaptically, could lead to an increase in the spontaneous postsynaptic current activities detected on the Purkinje cell.

To examine this mechanism, we added APV and CNQX to block excitatory transmission. This was without effect in the mutant (Fig. 2*A*). The excitatory transmission blockers had no effect on the current integral. Figure 2*B* shows the average result from these experiments. After APV and CNQX application, the current integral (averaged over a 3 min period) was not significantly different from the baseline (100%) before drug application: $103 \pm 9.8\%$ ($n = 15$, $p > 0.05$) for the wild type and $104 \pm 11.5\%$ ($n = 15$, $p > 0.05$) for the mutant. Collectively, these experiments suggest that the spontaneous postsynaptic current activity measured under our experimental conditions in both the wild type and the mutant had no excitatory component to it and was virtually all GABAergic in nature. The spontaneous currents are now referred to as sIPSCs in the following analysis. The chief effect of the Kv1.1 null mutation is to augment sIPSCs.

Kv1.1 null mutation selectively affects the frequency, but not amplitude, of the sIPSCs

Having established that the Kv1.1 null mutation augments sIPSCs (Fig. 1), we next determined what properties of sIPSCs are being affected. For example, the increase in the current integral of the mutant sIPSC over the wild type (Fig. 1*C*) could be explained by three factors: increase in the frequency of sIPSC events, prolongation of individual sIPSCs, or an increase in the amplitude of individual sIPSCs.

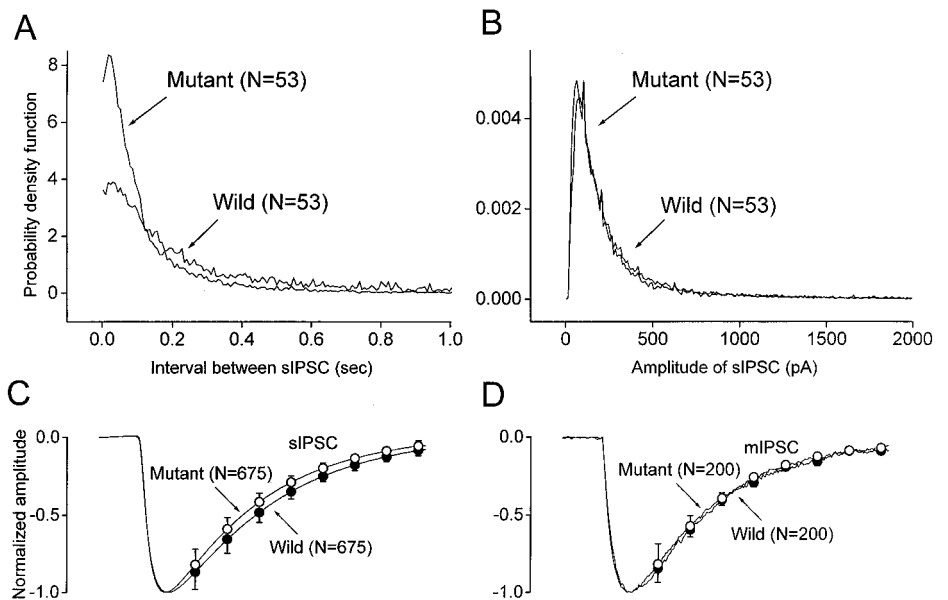
To elucidate which of these factors are affected by the Kv1.1 mutation, we subjected the sIPSC to detailed event analysis. Continuous segments, 3–5 min in length, of sIPSC recordings were analyzed to extract histograms for the peak amplitude and inter-event intervals for the sIPSCs. The histograms were converted to probability density functions for comparison between the mutant and wild-type data. Furthermore, individual sIPSCs that did not overlap with other events were selected at random and averaged together to form a composite sIPSC for shape comparison between the mutant and the wild type. The results of these analyses are shown in Figure 3*A, B* (distributions for the inter-event interval and amplitude), and *C* (shape comparison).

For the sIPSC amplitude distribution, two parameters that determine this distribution remained unaffected. The first parameter is the mean. It was 265.6 ± 27.7 pA ($n = 53$) in the wild type, which was not statistically different from the mutant value of 276.0 ± 26.3 pA ($n = 53$, $p > 0.05$). The second parameter is the variance-to-mean ratio. This ratio was 208.4 ± 29.1 pA in the wild type and was essentially unchanged at 202.2 ± 37.9 pA in the mutant ($n = 53$, $p > 0.05$). For the shape of the individual sIPSCs, no change was detected (Fig. 3*C*). The only change observed was in the distribution of the inter-event intervals or the frequency of the sIPSCs (Fig. 3*A*). The mean frequency of the sIPSCs nearly doubled, from a mean of 5.9 ± 0.7 sec $^{-1}$ ($n = 53$) in the wild type to 12.5 ± 1.6 sec $^{-1}$ ($n = 53$, $p < 0.001$) in the mutant.

Miniature IPSC is not affected

What mechanism might account for this specific increase in the frequency of sIPSC? Two different types of mechanisms can be considered. The first is a developmental mechanism. The developing nervous system is highly plastic, and alteration of K channel expression might lead to developmental changes. The increase in

Figure 3. Kv1.1 null mutation selectively affects the frequency (*A*) and not the amplitude (*B*) of the sIPSC. *A*, Probability density function for the inter-event intervals for mutant and wild-type sIPSC. Bin width in computing the probability density function was 0.007 sec. *B*, Probability density function for the amplitude of the mutant and wild-type sIPSC. Bin width in computing the probability density function was 10 pA. Data were compiled from age-matched null ($n = 53$ Purkinje cells from 27 animals) and wild-type littermates ($n = 53$ Purkinje cells from 27 animals). Mice ages were P10–P15. The distribution of the events (inter-event intervals or amplitude) was first compiled for each cell over 3–5 min of continuous recordings of the sIPSCs. The distribution was then converted into a probability density function for each cell. Then the probability density functions for 53 cells were averaged to yield a single averaged plot, as shown in *A* and *B*. *C, D*, Lack of effect of Kv1.1 null mutation on the shape of sIPSC (*C*) and mIPSC (*D*). Nonoverlapping events from the spontaneous current records of each phenotype were randomly selected, normalized with respect to the peak amplitude, and averaged. The sIPSC was recorded in normal saline solution. The mIPSC was recorded in saline solutions containing TTX ($1.0 \mu\text{M}$) to block spontaneous action potentials. For the sIPSC data: null data from 675 sIPSC events randomly selected from 27 mice; wild-type data from 675 sIPSC events from 27 mice. Age-matched null and wild-type littermates from P10–P15 mice. For the mIPSC data: null data from 200 mIPSC events randomly selected from eight mice; wild-type data from 200 mIPSC events from eight mice. Mice ages were P11–P14.



sIPSC frequency in the mutant could simply be attributable to an increase in the density of boutons produced by each basket cell (note that this is indistinguishable from an increase in the density of basket cells per Purkinje cell). Our patch pipette registers sIPSC coming from all basket cell innervation, and if the bouton density per basket cell or the density of basket cells per Purkinje cell increases in the mutant, the frequency of sIPSC will increase. The second possibility is a direct alteration of the membrane excitability of the basket cells caused by deletion of Kv1.1 (known to be normally localized on the axonal arborization). For example, basket cells are known to be spontaneously active (i.e., firing action potentials). If this spontaneous firing rate is increased by the Kv1.1 mutation, the sIPSC frequency detected on the Purkinje cell would increase.

To distinguish between these two types of mechanisms, we measured spontaneous miniature IPSC (mIPSC) by adding TTX to block action potentials. Experiments were performed in the presence of APV ($100 \mu\text{M}$) and CNQX ($10 \mu\text{M}$) to block excitatory transmissions. Figure 4*A, B* (left) first shows the sIPSC in a mutant and in an age-matched wild-type slice before $1.0 \mu\text{M}$ TTX application. For these two particular cells, the frequency of the mutant sIPSC was 14.3 sec^{-1} , which was larger than the frequency of 7.7 sec^{-1} for the wild-type cell. After TTX ($1.0 \mu\text{M}$) was added (right), there was a marked reduction in both the amplitude and frequency of the events of each genotype. Interestingly, the resultant mIPSC in the two cells became indistinguishable, with the frequency of the two becoming virtually identical (3.0 sec^{-1} in mutant and 3.4 sec^{-1} in wild type). Figure 4*C, D* shows the average result of the amplitude and inter-event distribution for the mIPSC for the wild type and the mutant. The distributions were virtually identical. For the mIPSC amplitude distributions, both the mean ($68.6 \pm 4.7 \text{ pA}$ in mutant; $68.1 \pm 5.4 \text{ pA}$ in the wild type; $n = 15$, $p > 0.05$) and the variance-to-mean ratio ($19.4 \pm 4.3 \text{ pA}$ in mutant; $20.6 \pm 4.4 \text{ pA}$ in wild type; $n = 15$, $p > 0.05$) were not statistically different. Likewise, the frequency of the mIPSC was not significantly different, being $1.58 \pm$

0.25 sec^{-1} ($n = 15$) for the mutant, and $1.23 \pm 0.23 \text{ sec}^{-1}$ for the wild-type ($n = 15$, $p > 0.05$). Figure 3*D* shows that the shape of individual mIPSC was not affected by the mutation.

If the Kv1.1 mutation led to a change in basket cell innervation pattern (i.e., increase in the number of basket cells per Purkinje cell), then both the mIPSC and the sIPSC should be similarly affected. That there is a selective effect on sIPSC (Fig. 3*A*) but not on mIPSC (Fig. 4*D*) strongly argues against a change in the basket cell innervation pattern in the mutant. Our data thus far clearly implicate a change in the excitability of the presynaptic cell, the basket cell. Where is the locus of excitability change on the basket cell?

Firing rate of basket cells is not affected

One simple mechanism to account for the increase in the sIPSC frequency is an increase in the spontaneous firing rate of the basket cells. We therefore used cell-attached recordings to measure spontaneous action currents at the cell soma of basket cells. Figure 5 shows typical cell-attached recordings of the basket cell action currents from wild-type and age-matched mutant mice. The rate of spontaneous action currents in basket cells was not affected by the Kv1.1 mutation (Fig. 5*C*), being $7.1 \pm 1.0 \text{ sec}^{-1}$ ($n = 37$) in the mutant, which is not statistically different from the value of $6.6 \pm 1.0 \text{ sec}^{-1}$ ($n = 34$, $p > 0.05$) in the wild type.

Evoked IPSC does not show repetitive activity

If the firing rate of basket cells was not affected, what causes the sIPSC frequency to increase in the mutant? One mechanism is that after Kv1.1 deletion, each action potential generates multiple IPSC responses. We therefore used evoked IPSCs to examine whether multiple IPSC activity follows a single stimulation in the mutant. A fine-tip bipolar stimulating electrode was placed within the inner one-third of the molecular layer to elicit evoked IPSC in a Purkinje cell. Excitatory transmission was blocked by CNQX and APV. Stimulation was increased from 10 to 100 V, but only stimulation at 80 V, which was near maximal stimulation, was

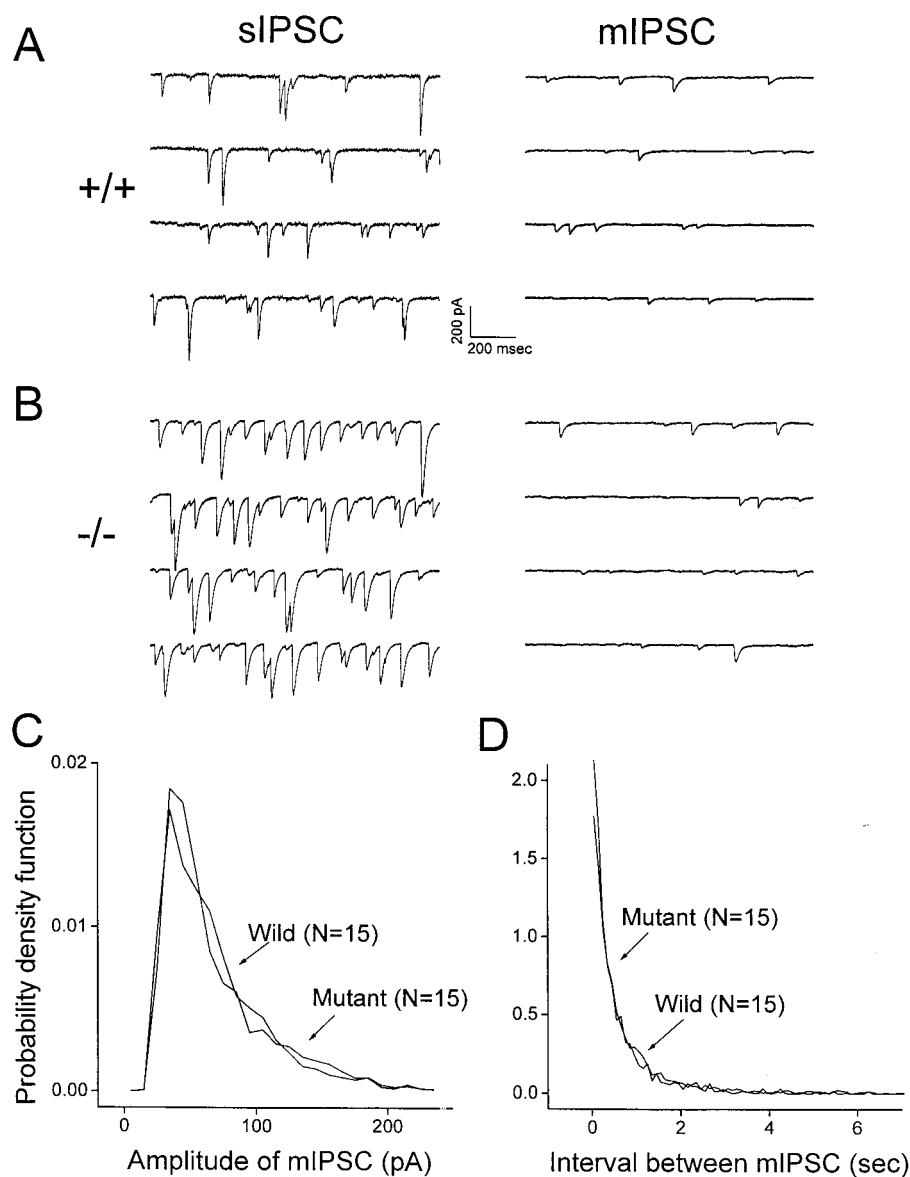


Figure 4. Kv1.1 null mutation selectively affects the frequency of sIPSC but not mIPSC. *A, B (left)* sIPSC from a wild-type (*A*) and a null Purkinje cell (*B*) before TTX ($1.0 \mu\text{M}$). Note the higher frequency of sIPSC in the mutant as compared with the wild-type. *A, B (right)*, The mIPSC obtained from the same cells after TTX application. Note that the frequency of mIPSC was virtually identical in the two cells. *C, D*, The average results of the mIPSC data. *C* shows the probability density function for the amplitude, and *D* shows the probability density function for the inter-event intervals ($n = 15$ cells for each phenotype). Notice that both the amplitude and the inter-event interval distributions for mIPSC were not affected by the Kv1.1 mutation. Bin width was 10 pA for the amplitude distribution, and 0.1 sec for the inter-event interval distribution. Ages were P10–P15.

analyzed. At 80 V stimulation, each experiment consisted of 50 single stimulations given every 2 sec. The result from a mutant is shown in Figure 6. Figure 6*A* shows six traces showing the evoked response superimposed on background spontaneous activity. The amplitude of the evoked IPSC varied considerably in repeated stimulation, as has already been reported in normal slices (Vincent et al., 1992). Despite the varying pattern of the background spontaneous activity, survey of the individual traces did not reveal poststimulation multiple discharges that correlated with the stimulation. Two quantitative means were further used to examine this point. First, we stacked all 50 traces together (Fig. 6*B*) and calculated the ensemble average (Fig. 6*C*). We then selected 3 of the 50 traces in which the evoked IPSC response is devoid of overlapping spontaneous events for the first 60 msec (an example is the fifth trace in Fig. 6*A*). We then calculated the average of these three traces, starting at the stimulation artifact and ending 60 msec later. This average segment represents the shape of an evoked response that does not exhibit repetitive discharge during its early phase. We next asked the following

question: does the average behavior of the 50 traces reflect the sum of an evoked response consisting of a single IPSC superimposed on random background sIPSC activity? To answer this question, we calculated the average of the baseline spontaneous activity *before* stimulation and predicted the behavior *after* stimulation by adding to this average a scaled version of the evoked response based on the three traces. The result is shown as the smooth trace in Figure 6*C*. We can now compare the smooth trace and the ensemble average of the 50 traces *after* stimulation. This comparison (Fig. 6*C*) demonstrates that the poststimulation behavior is well fitted by the sum of random prestimulation activity plus an evoked response that elicits only a single IPSC. For example, the ensemble average of the poststimulation activity, starting 60 msec second after the stimulation (the time at which the evoked response is mostly over) and ending at 600 msec after the stimulation, is identical to the ensemble average of the spontaneous activity before the stimulation. Similar analysis applied to the wild-type slice reached the same conclusion (Fig. 6*D–F*). The averaged peak of the evoked response is 435.9 ± 64.7

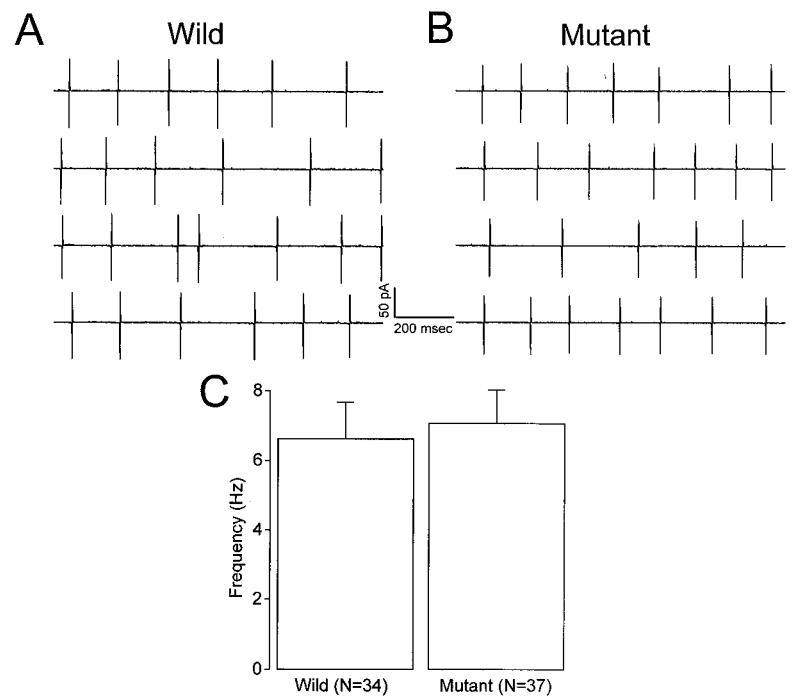


Figure 5. Kv1.1 null mutation does not alter basket cell firing rate. Cell-attached recordings of spontaneous action currents were made at the cell body of basket cells from the inner one-third of the molecular layer. Representative recordings from a wild-type (*A*) and mutant (*B*) basket cell are shown. *C* shows the average action current frequency calculated from 2 min of continuous recordings in each experiment. Data from five wild-type ($n = 34$ cells) and five age-matched mutant mice ($n = 37$ cells; P10–P15). The averages are not statistically different.

pA ($n = 10$) in the wild type, which is not statistically different from that of 547.8 ± 103.4 pA ($n = 13$, $p > 0.05$) in the mutant. Furthermore, with the amplitude normalized to the same value, the shape of the averaged evoked response is the same for both the mutant and the wild type (Fig. 6*G*).

For the second quantitative method to evaluate whether the evoked IPSC is followed by repetitive activity, we measured the average event frequency over a 400 msec segment before and after the stimulation. The results (Fig. 7*C*) reveal no significant difference between the prestimulation and poststimulation event frequency. Finally, Vincent et al. (1992; their Fig. 7) reported double synaptic events in which the evoked response consisted of two closely spaced events [also see Auger et al. (1998)]. To determine whether there might be more occurrences of these double synaptic events in the mutant, we first computed the event frequency over a 50 msec segment before the stimulation. We then computed the event frequency over a 50 msec segment immediately after the stimulation, minus one event associated with the stimulation. There is no significant difference between these two event frequencies (Fig. 7).

In summary, our evoked IPSC analysis suggests that the increase in frequency of sIPSC in the mutant cannot be accounted for by multiple IPSCs evoked by a single basket cell action potential. This, coupled with an unaltered basket cell firing rate, suggests that the locus of hyperexcitability in the mutant basket cell lies downstream from the cell body and upstream from the boutons. The simplest mechanism, as examined in Discussion, is that Kv1.1 deletion alters the likelihood of action potentials arriving at the nerve terminal.

Effects of potassium channel blockers on wild-type slices

If the change in sIPSC in the mutant reflects a direct role of Kv1.1 in modulating the excitability of the basket cells, then we should be able to reproduce key features of the mutant phenotype by pharmacological block of Kv1.1 in wild type. In mammalian cell

lines that have been transfected with Kv1.1 (Grissmer et al., 1994), the Kv1.1 homomultimeric channels are blocked by 4-AP ($K_d \sim 290 \mu\text{M}$), TEA ($K_d \sim 0.3$ mM), and DTX ($K_d \sim 20$ nM). We therefore tried some of these blockers on wild-type slices, keeping the concentrations lower than or at the K_d values to minimize nonspecific block of other K channel subtypes.

The result for 4-AP (0.3 mM) is shown in Figure 8. Figure 8*A* shows a plot of the current integral of sIPSCs (over evenly spaced 1.23 sec segments) for a single wild-type cell before and after 4-AP application. There was a transient increase in the current integral that was followed by a slowly declining response. Adding APV and CNQX on top of 4-AP did not change this latter response, suggesting that the slowly declining response elicited by 4-AP did not contain any excitatory component (Fig. 8*A*). The initial transient response in 4-AP also lacked an excitatory component, because it was also present when APV and CNQX were added before 4-AP was applied (Fig. 8*B*). The response elicited by 4-AP was completely blocked by bicuculline (Fig. 8*A,B*). We conclude that 4-AP, at this low concentration of 0.3 mM, selectively blocks a subset of K channels that normally controls GABAergic inhibition. Does 4-AP mimic the mutant phenotype in producing a specific effect on the sIPSC frequency but not its amplitude?

Figure 8*E,F* shows the distributions of the inter-event intervals (*E*) and amplitudes (*F*) calculated from the same group of cells before and after 0.3 mM 4-AP application. By comparison with the mutant data (Fig. 3*A,B*), it is clear that 4-AP reproduced the key phenotype of the mutant in its selective effect on the sIPSC frequency. Application of 4-AP increased the mean frequency of the wild-type sIPSCs (Fig. 8*E*) from 3.5 ± 0.8 sec⁻¹ to 7.0 ± 1.3 sec⁻¹ in the same cells tested ($n = 4$, $p < 0.05$). In contrast, the mean sIPSC amplitude (Fig. 8*F*) was not affected (370.1 ± 61.8 pA before 4-AP and 386.7 ± 104.1 pA after 4-AP; $n = 4$, $p > 0.05$).

Figure 9 (*left*) summarizes the average results in wild-type

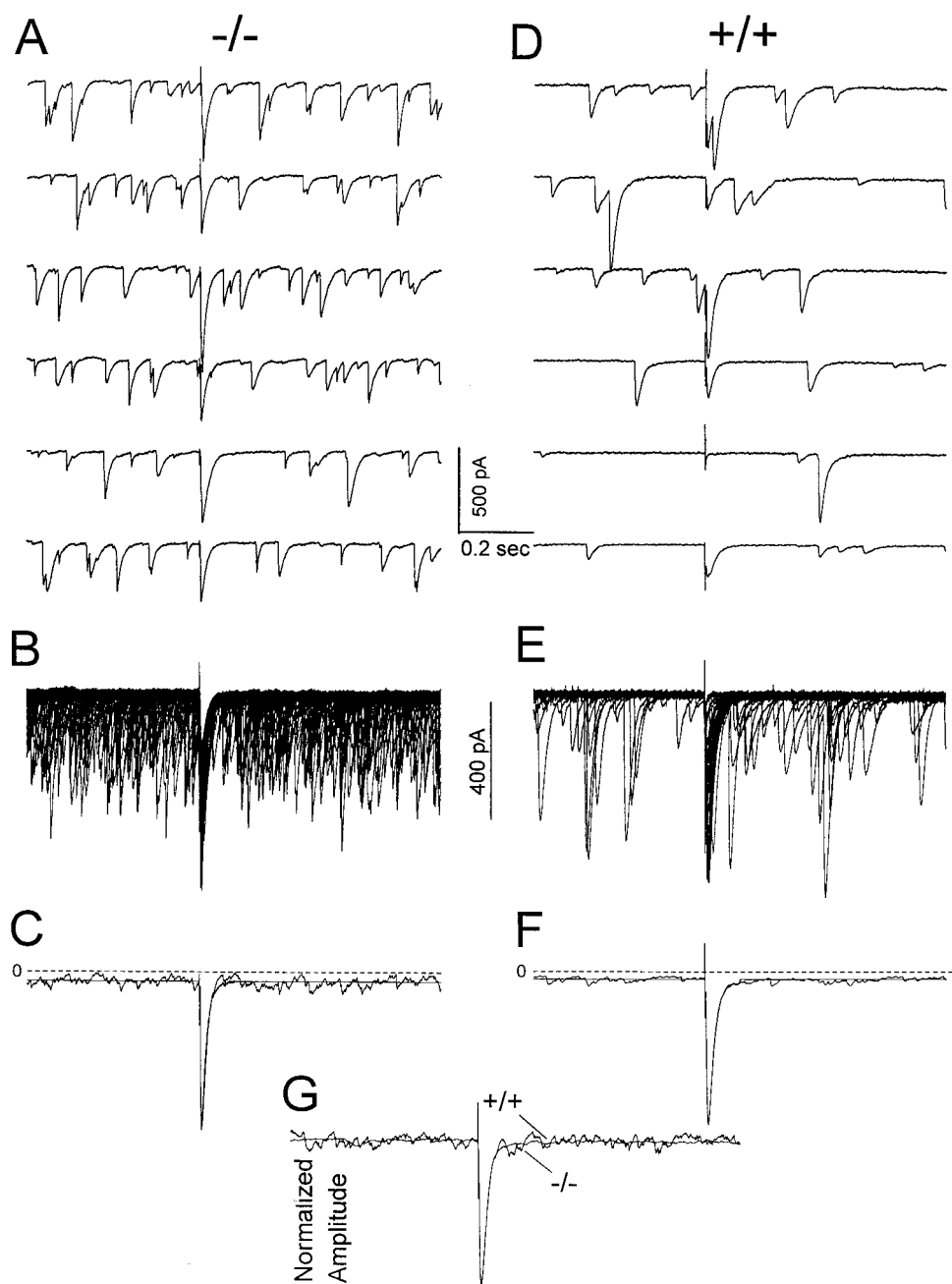


Figure 6. Evoked responses in mutant (*left*) and wild-type (*right*) Purkinje cells. Evoked IPSC responses were elicited by extracellular stimulation of the inner one-third of the molecular layer where the basket cells reside. *A* shows six traces from an ensemble of 50 traces, each evoked by a single stimulation of 80 V. Stimulation was applied every 2 sec. Results are from a P13 mutant mouse. *B* shows the superimposition of the 50 traces; *C* shows the ensemble average of the 50 traces. The smooth trace was calculated as described in Results. *D–F* show similar analysis performed on a wild-type Purkinje cell from a P13 wild-type mouse. *G* compares the shape of the average evoked response from the mutants ($n = 13$ cells) and the wild type ($n = 10$ cells). The background spontaneous activity was subtracted before display. The amplitude of the two evoked responses has been normalized to the same peak amplitude.

slices for all of the blockers examined (4-AP = 0.3 mM; DTX = 8 nM; TEA = 0.3 mM). In all cases, the K channel blockers were added to normal saline solutions, and the fractional change in the amplitude and the frequency of the spontaneous currents was measured. Although the solutions contained no excitatory transmission antagonists, we assumed that only GABAergic responses were elicited by the K channel blockers at these low concentrations because the response in the presence of K channel blockers was completely eliminated by bicuculline. Figure 9 (*left*) shows that in the wild-type slices, these K channel blockers selectively increased the sIPSC frequency (*top*) and not its amplitude (*bottom*). Hence, the hallmark of the Kv1.1 null phenotype was reproduced in the wild-type slices by these K channel blockers, at least in these low concentrations of blockers that were used.

Residual sensitivity of the mutant to Shaker channel blockers

An interesting issue is whether Kv1.1 is the *only* K channel subtype that modulates GABAergic inhibition. We therefore applied K channel blockers (4-AP, TEA, and DTX) to the mutant slices to determine whether the sensitivity of sIPSC to K channel blockers was abolished and to compare the results with those from the wild type. Figure 8*C,D* shows that 4-AP (0.3 mM) produced in the mutant a selective increase in GABAergic inhibition qualitatively similar to that produced in the wild type. Figure 9 (*right*) summarizes the results of K channel blockers on the mutant. Interestingly, residual effects of K channel blockers were still present for 4-AP and DTX but not for TEA. In the case of 4-AP and DTX, the response elicited by these drugs was still

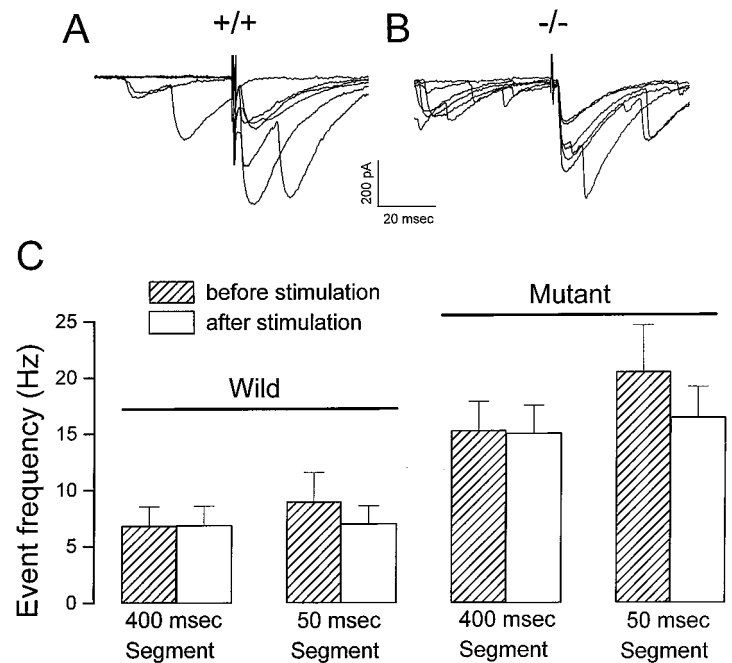


Figure 7. Analysis of the event frequency before and after stimulation. *A* and *B* show events over a 50 msec segment before and after stimulation. *C* shows the measured event frequency over 50 or 400 msec segments before and immediately after stimulation. For the 50 msec segments, the counts of the poststimulation events did not include the single event associated with the stimulation. The prestimulation and poststimulation event frequency were not statistically different ($p > 0.05$) for both the wild type ($n = 10$) and mutant ($n = 13$).

characterized by a selective increase of frequency over amplitude. In the case of TEA, the Kv1.1 null mutation appears to have eliminated the TEA response, at least at 0.3 mM.

It is interesting that after Kv1.1 deletion, 4-AP still produced a similar and even larger fractional effect on the sIPSC frequency in the mutant. One possibility is that the residual K channels in the mutant have a higher 4-AP sensitivity than the wild type. This might arise, for example, if Kv1.1 deletion causes a change the subunit composition of the residual heteromultimeric K channels, causing a shift in their 4-AP sensitivity.

Collectively, the simplest interpretation of these results is that other Shaker-type K channels (such as Kv1.2) remain in the Kv1.1 mutant that still contribute to control of GABAergic inhibition. However, it is also clear that these residual K channels cannot fully compensate for the loss of Kv1.1. Indeed, a TEA-sensitive component in the endogenous K currents appears to have been selectively abolished.

Behavioral studies on motor skill

We have previously shown that the Kv1.1 mutant mice, when forced to swim in cold water, exhibited an inability to maintain axial orientation near the end of a 2 min swim, followed by generalized body tremors. We now test the ability to maintain balance in a more physiological setting.

Two behavioral tests (stationary thin rod and rotarod) were used. Mutant mice (21–32 d old) and age-matched wild-type littermate controls were used. All tests were performed with the investigator blinded to the genotype. In the stationary thin rod test (Fig. 10*B*), mutants showed a significantly shorter retention time than the wild type in 3 consecutive test days. Furthermore, because the Kv1.1 mutants are predisposed to spontaneous epileptic activities (Smart et al., 1998), an important issue is whether spontaneous seizures might occur while the mice are on the thin rod, causing the mice to fall. We therefore performed simultaneous EEG measurements on mice undergoing the thin rod test for both mutants ($n = 10$) and wild-type mice ($n = 11$). We considered it important to perform EEG measurements on the wild-type mice because we wanted to rule out the added weight of

the electrodes and the connecting wire in causing mice to fall. In these experiments, we detected no epileptic activities, both before and during the brief stay on the stationary thin rod, that could explain the shortened retention time in this test. These results were averaged together with those obtained without EEG measurements and are displayed in Figure 10*B*.

In the second test (rotarod), the mice had to actively walk to stay on the thicker but rotating rod. In this test, interestingly, the mutants failed to show a defect in their ability to remain on the rotating rod (Fig. 10*A*). Collectively, our results suggest that only certain motor skills, such as those needed to maintain axial balance, are selectively affected by the Kv1.1 null mutation.

DISCUSSION

This paper identifies, through a combined approach of gene deletion and electrophysiological studies, a specific K channel subtype (Kv1.1) as a major determinant of the spontaneous GABAergic inhibition of Purkinje cells in the cerebellum. The function of Kv1.1 is highly specific: it modulates only the frequency and not the amplitude or shape of the sIPSC. The mIPSC remains unchanged; nor is the spontaneous firing rate of basket cells affected. Spontaneous excitatory transmission appears unperturbed. Residual K channel genes cannot fully compensate for the functional loss of this single gene. Kv1.1 null mice show a subtle defect in fine motor skills, as exemplified by a compromised ability to maintain balance on a thin stationary rod. Our finding is consistent with the known localization of Kv1.1 to the basket cell axonal arborization that embraces the Purkinje cell, a strategic position to modulate the final balance in the excitatory and inhibitory signal integration of the only efferent output from the cerebellum.

How does the Kv1.1 null mutation augment GABAergic current activities on the Purkinje cell body?

Four distinct mechanisms could account for the increase in sIPSC detected at the Purkinje cell soma. These mechanisms are (1) an

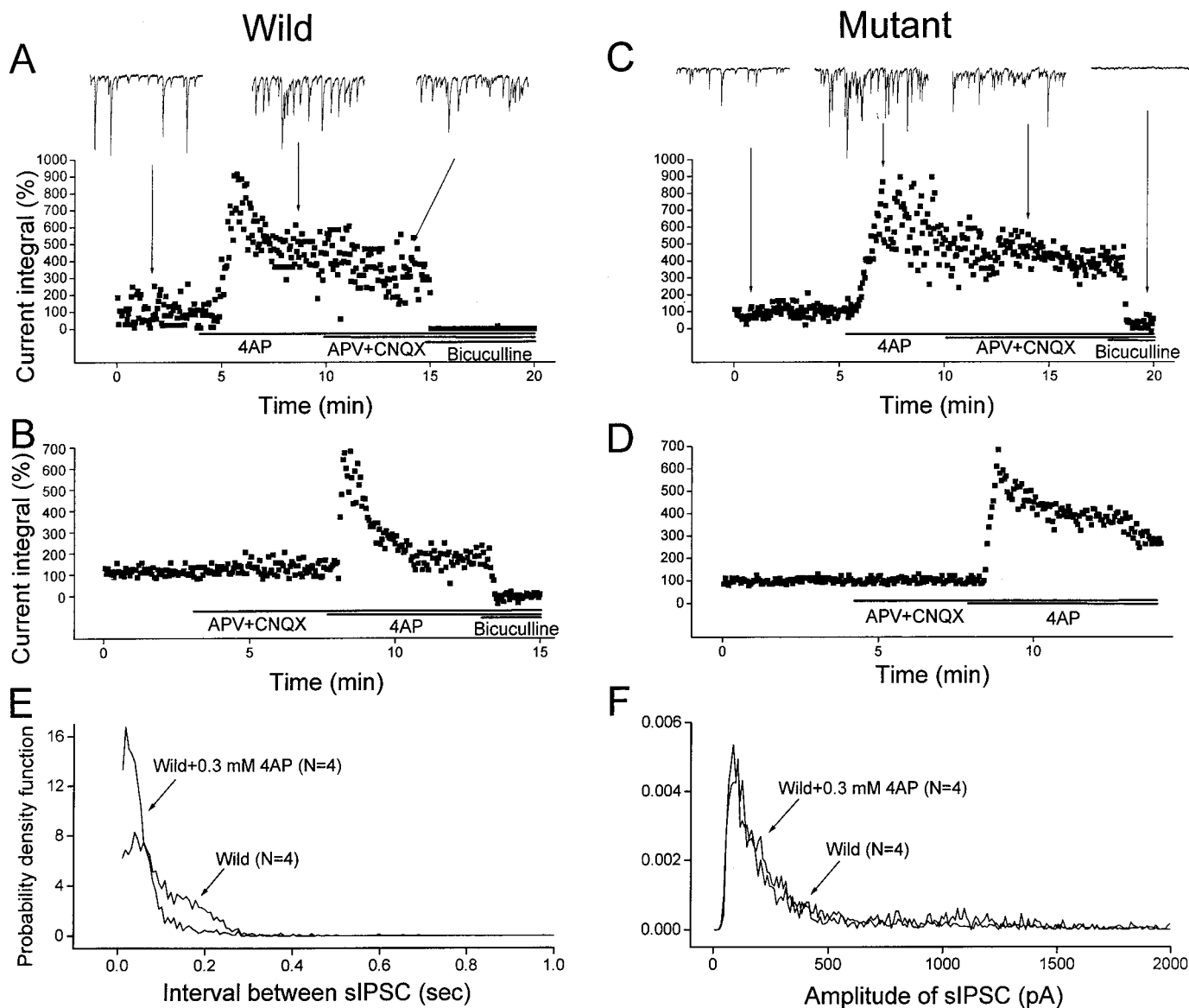


Figure 8. Effect of 4-AP on the wild-type and null sIPSC. *A* shows the effect of 4-AP (0.3 mM) on sIPSC from a wild-type cell, followed by application of excitatory transmission blockers [APV (100 μ M) and CNQX (10 μ M)] and bicuculline (10 μ M) to verify the inhibitory nature of the response evoked by 4-AP. *B* shows that a similar result (from a different wild-type cell) was obtained if APV and CNQX were applied *before* 4-AP application. *C* and *D* show similar experiments performed on sIPSC from a mutant Purkinje cell. In all cases, the current integral of sIPSC was used to monitor the effects of the drug application. Representative current traces are shown at the indicated times. *E*, *F*, 4-AP selectively affects the frequency (*E*), but not amplitude (*F*), of wild-type sIPSC. Probability density functions for the inter-event interval (*E*) and amplitude (*F*) were computed for the sIPSC from the same wild-type cells before and after 4-AP (0.3 mM) application. Bin width was 0.007 sec in *E* and 10 pA in *F*. Note that only the frequency (inter-event interval distribution) was affected. This selective effect of 4-AP on the frequency of the wild-type sIPSC mimics the selective effect on the frequency of sIPSC produced by the Kv1.1 null mutation (see Fig. 3*A,B*).

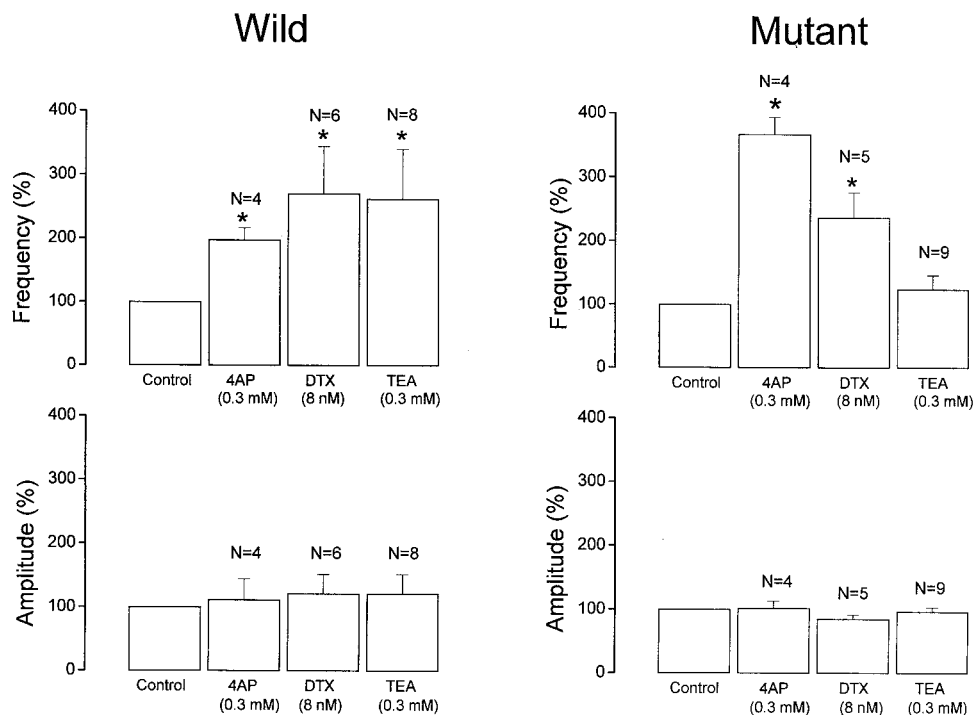
increase in excitatory drive to basket cells, (2) a change in basket cell innervation on the Purkinje cell because of developmental plasticity, (3) an upregulation of GABA_A receptors on the Purkinje cell, and (4) an increase in the excitability of the basket cells. Mechanisms 1 and 2 have been discussed in Results and are considered unlikely. The possibility of an upregulation of GABA_A receptors on the Purkinje cell is also considered unlikely. First, the amplitude of sIPSC is unaffected, which is the opposite of that expected if there were an increase in GABA_A receptor density. Second, it is unclear how an increase in GABA_A receptor density could produce a change in the frequency that is selective only for sIPSC and not for mIPSC. This leaves the

fourth possibility, which is that Kv1.1 deletion enhances the excitability of the basket cell. The locus of the excitability change is specific, as discussed below.

The locus of excitability change on the basket cell is downstream from the cell body and upstream from the boutons

Figure 1*D* shows a scheme of a basket cell with a cell body and a single axon that gives off a descending collateral to embrace the Purkinje cell with several boutons. This scheme is based on a 13-d-old biocytin-filled basket cell from Llano et al. (1997). Deletion of Kv1.1 could enhance excitability of the basket cell at

Figure 9. Summary data on the effects of K channel blockers on the frequency and amplitude of wild-type (*left*) and mutant (*right*) sIPSC. For each parameter (amplitude or frequency), we calculated, for the same cell, the *fractional* change in its value before and after the drug application. Each experiment consisted of a baseline recording of sIPSC for 15 min followed by 15 min of drug application. Event analysis was performed to extract sIPSC amplitude and inter-event intervals for each of the 15 min segments. Bath concentrations of drugs used are as follows: 4-AP (0.3 mM), DTX (8 nM), and TEA (0.3 mM). * denotes that the values were different from the control values at a statistically significant level of $p < 0.05$ using a paired two-population *t* test from the software Origin. Note that all other values shown are not significantly different from the control, including all of the amplitude data, and *in particular*, the frequency data for TEA in the mutant.



three sites: the basket cell body, the boutons, and the branch points or axonal arborizations that precede the boutons.

Basket cell firing rate

Basket cells generate spontaneous action potentials (Midgaard, 1992; Llano and Gerschenfeld, 1993; Vincent and Marty, 1996). A doubling of the basket cell firing rate would explain the doubling of sIPSC frequency. However, the Kv1.1 null mutation does not change the basket cell firing rate (Fig. 5). Our basket cell recordings are also consistent with recent findings by Southan and Robertson (1998) that DTX-sensitive K channels (including presumably Kv1.1) are absent from the basket cell body. Hence, the increase in sIPSC frequency in the mutant must occur via a mechanism located downstream from the cell body.

Bouton excitability

There are various scenarios by which the excitability of the boutons could be elevated in the mutant.

Increased evoked release probability. If Kv1.1 is located on the presynaptic membrane, its deletion will broaden the action potential. This will increase the evoked release probability. This, in turn, will reduce the number of failures, causing an increase in the event frequency. There are compelling arguments against this scenario. For most models of synaptic release (except the case of a synaptic connection with one release site), an increase in the evoked release probability should also change the skew of the event amplitude distribution as well as increase the mean amplitude of the successful events. The basket cell–Purkinje cell connection satisfies a multisite release, because the mean amplitude of mIPSC is about three times smaller than that of the sIPSC. Given this, an increase in release probability is unlikely, because the shape of the sIPSC amplitude distribution (the successful events), including its mean and variance, is totally unaffected by the mutation (Fig. 3B). This, coupled with the unaltered mean and variance of the mIPSC amplitude distribution (Fig. 4C),

suggests that the mean quantal content and the quantal size may also be unaffected by the mutation.

Repetitive IPSC discharge. The boutons in the mutant may be hyperexcitable, allowing an action potential to trigger multiple IPSC responses. However, evoked IPSC did not show repetitive discharge in the mutant (Figs. 6, 7). Alternatively, Kv1.1 might cause a depolarization of the bouton resting potential, rendering the bouton hyperexcitable. The fact that the frequency of mIPSC, which is known to be sensitive to the resting potential, is unaffected argues against this possibility. Taken together, our data give no indication that Kv 1.1 deletion alters the excitability of the boutons.

Branch point failures

The unaltered basket cell firing rate, coupled with the preservation of one-to-one evoked response after Kv1.1 deletion, suggests that the locus for the increased excitability lies downstream from the cell body and upstream from the boutons. The simplest explanation of our data is that there is an increased likelihood of action potentials reaching the nerve terminal. The affected locus is likely the branch points or the axonal swelling that is sometimes seen (Llano et al., 1997, their Fig. 5). Branch points or axonal swellings are sites of low safety for nerve conduction because of impedance mismatch. If Kv1.1 is localized at or near the branch points, it may regulate conduction failures. For example, deletion of Kv1.1 should strengthen the inward sodium currents and improve the safety factor to enhance propagation past the branch points. Consequently, for a given rate of spontaneous firing generated upstream, more action potentials get past the axonal branch points and invade the boutons. This hypothesis is attractive for several reasons. First, Kv1.1 has a unique localization at septate-like junctions within the axonal arborization that precedes the nerve terminal (Wang et al., 1994, their Fig. 5c). Second, regulation of neurotransmission via modulation of branch point excitability has been recognized (Barron and Mat-

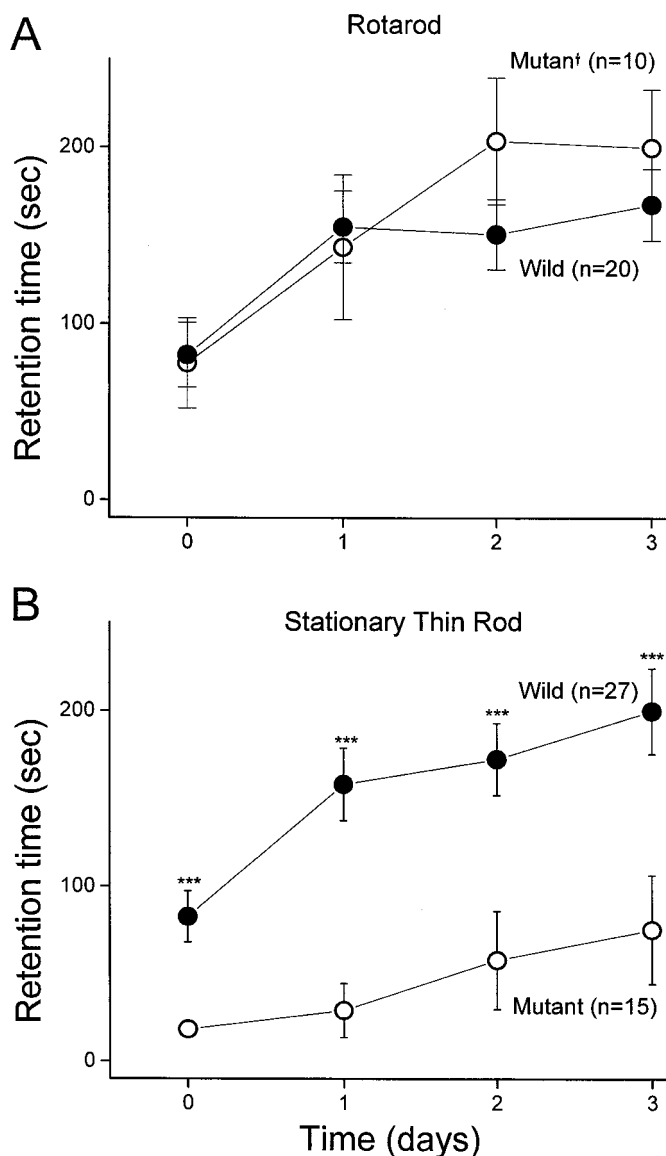


Figure 10. Motor skills tests on wild-type and Kv1.1 null mutant mice. *A* shows retention time on a rotarod; *B* shows retention time on a thin stationary rod. The same mice were tested on consecutive days. *** denotes mutant values that were statistically different from the wild-type values at $p < 0.001$. The shorter retention time of the mutant on the thin stationary rod was not caused by a heavier body weight, because the body weights of the two groups of mice were not significantly different, being 9.8 ± 2.4 gm in the mutant ($n = 15$) and 11.1 ± 3.0 gm in the wild-type ($n = 27$, $p > 0.05$).

thews, 1935; Krnjevic and Miledi, 1959; Grossman et al., 1973; Deschenes and Landry, 1980). Recently, Vincent and Marty (1996) suggested that random branch point failures in the basket cells may account for the large variance in the amplitude of the evoked IPSC. In paired recordings of pyramidal cells in hippocampal slice cultures, Debanne et al. (1997) demonstrated that a fast-inactivating, A-type K channel may be involved in presynaptic action potential failures at axonal branch points.

The main effect of the mutation appears to increase the likelihood of conduction past a branch point that controls the same group of boutons downstream from that branch point. In Figure 1*D*, the likely loci are either the main collateral branch point or

the axonal swelling. At these loci, a reduction in action potential failure rate will increase the sIPSC frequency without affecting the shape (mean and variance) of the successful event amplitude. A further test of this hypothesis will require analysis of failures in evoked IPSC in paired recordings from Purkinje and basket cells. Extracellular stimulation, as performed in this study, suffers from the uncertainties that the branch points may be directly stimulated and that we have no direct monitoring of successful axonal stimulation.

Deficits in motor skill

The Kv1.1 null mice show a defect in ability to maintain balance on a thin stationary rod. It is possible that an abnormal shift in the GABAergic tone (i.e., elevated in the Kv1.1 mutant) shifts the overall balance between excitatory and inhibitory signal integration in the cerebellum, thus contributing to inability to maintain axial balance. Interestingly, stress appears to exacerbate the severity of axial balance defects, as revealed by the inability of the mutant mice to remain upright during a swim in cold water (Zhou et al., 1998). Catecholamines have been shown to modulate GABAergic activity in the cerebellum (Llano and Gerschenfeld, 1993). CNS transmission is temperature sensitive (Hartingham and Larkman, 1998), and conduction at branch points is particularly sensitive to temperature changes (Westerfield et al., 1978). Kv1.1 deletion might make the conduction failures at branch points very sensitive to temperature changes.

REFERENCES

- Auger C, Kondo S, Marty A (1998) Multivesicular release at single functional synaptic sites in cerebellar stellate and basket cells. *J Neurosci* 18:4532–4547.
- Barron DH, Matthews BHC (1935) Intermittent conduction in the spinal cord. *J Physiol (Lond)* 85:73–103.
- Browne DL, Ganchar ST, Nutt JG, Brunt ERP, Smith EA, Kramer P, Litt M (1994) Episodic ataxia/myokymia syndrome is associated with point mutations in the human potassium channel gene, KCNA1. *Nat Genet* 8:136–140.
- Debanne D, Guerineau NC, Gahwiler BH, Thompson SM (1997) Action-potential propagation gated by an axonal I_A -like K conductance in hippocampus. *Nature* 389:286–289.
- Deschenes M, Landry P (1980) Axonal branch diameter and spacing of nodes in the terminal arborization of identified thalamic and cortical neurones. *Brain Res* 191:538–544.
- Eccles JC, Ito M, Szentagothai J (1967) The cerebellum as a neuronal machine. Berlin: Springer.
- Grissmer S, Nguyen AN, Aiyar J, Hanson DC, Mather RJ, Gutman GA, Karmilowicz MJ, Auperin DD, Chandy KG (1994) Pharmacological characterization of five cloned voltage-gated K channels, types Kv1.1, 1.2, 1.3, 1.5, and 3.1, stably expressed in mammalian cell lines. *Mol Pharmacol* 45:1227–1234.
- Grossman Y, Spira ME, Parnas I (1973) Differential flow of information into branches of a single axon. *Brain Res* 64:379–386.
- Hartingham NR, Larkman AU (1998) The reliability of excitatory synaptic transmission in slices of rat visual cortex in vitro is temperature dependent. *J Physiol (Lond)* 507:1:249–256.
- Kim JJ, Thompson RF (1997) Cerebellar circuits and synaptic mechanisms involved in classical eyeblink conditioning. *Trends Neurosci* 20:177–181.
- Konnerth A, Llano I, Armstrong CM (1990) Synaptic currents in cerebellar Purkinje cells. *Proc Natl Acad Sci USA* 87:2662–2665.
- Korn H, Faber DS (1980) Electrical field effect interactions in the vertebrate brain. *Trends Neurosci* 3:6–9.
- Krnjevic K, Miledi R (1959) Presynaptic failure of neuromuscular propagation in rats. *J Physiol (Lond)* 149:1–22.
- Laube G, Roper J, Pitt JC, Sewing S, Kistner U, Garner CC, Pongs O, Veh RW (1996) Ultrastructural localization of Shaker-related potassium channel subunits and synapse-associated protein 90 to septate-like junctions in rat cerebellar pinceaux. *Mol Brain Res* 42:51–61.
- Llano I, Gerschenfeld HM (1993) β -adrenergic enhancement of inhibi-

- tory synaptic activity in rat cerebellar stellate and Purkinje cells. *J Physiol (Lond)* 468:201–224.
- Llano I, Marty A, Armstrong CM, Konnerth A (1991) Synaptic- and agonist-induced excitatory currents of Purkinje cells in rat cerebellar slices. *J Physiol (Lond)* 434:183–213.
- Llano I, Tan YP, Caputo C (1997) Spatial heterogeneity of intracellular Ca signals in axons of basket cells from rat cerebellar slices. *J Physiol (Lond)* 502.3:509–519.
- McNamara NMC, Muniz ZM, Wilkin GP, Dolly JO (1993) Prominent location of a K channel containing the α -subunit Kv1.2 in the basket cell nerve terminals of rat cerebellum. *Neuroscience* 57:1039–1045.
- McNamara NMC, Averill S, Wilkin GP, Dolly JO, Priestley JV (1996) Ultrastructural localization of a voltage-gated K channel α -subunit (Kv1.2) in the rat cerebellum. *Eur J Neurosci* 8:688–699.
- Midgaard J (1992) Stellate cell inhibition of Purkinje cells in the turtle cerebellum in vitro. *J Physiol (Lond)* 457:355–367.
- Ramon y Cajal S (1911) *Histologie du système nerveux de l'homme et des vertèbres*. Paris: Maloine.
- Rhodes KJ, Keilbaugh SA, Battezueta NX, Lopez KL, Trimmer JS (1995) Association and colocalization of K channel α - and β - subunit polypeptides in rat brain. *J Neurosci* 15:5360–5371.
- Rhodes KJ, Monaghan NM, Barrezaeta NX, Nawoschick S, Bekele-Arcuri Z, Matos MF, Nakahira K, Schechter LE, Trimmer JS (1996) Voltage-gated K channel β subunits: expression and distribution of Kv β 1 and Kv β 2 in adult rat brain. *J Neurosci* 16:4846–4860.
- Smart SL, Lopantsev V, Zhang CL, Robbins CA, Wang H, Chiu SY, Schwartzkroin PA, Messing A, Tempel BL (1998) Deletion of the Kv1.1 potassium channel causes epilepsy in mice. *Neuron* 20:809–819.
- Southan AP, Robertson B (1998) Patch-clamp recordings from cerebellar basket cell bodies and their presynaptic terminals reveal an asymmetric distribution of voltage-gated potassium channels. *J Neurosci* 18:948–955.
- Veh RW, Lichtinghagen R, Sewing S, Wunder F, Grumbach IM, Pongs O (1995) Immunohistochemical localization of five members of the Kv1 channel subunits: contrasting subcellular locations and neuron-specific co-localizations in rat brain. *Eur J Neurosci* 7:2189–2205.
- Vincent P, Marty A (1996) Fluctuations of inhibitory postsynaptic currents in Purkinje cells from rat cerebellar slices. *J Physiol (Lond)* 494:183–199.
- Vincent P, Armstrong CM, Marty A (1992) Inhibitory synaptic currents in rat cerebellar Purkinje cells: modulation by postsynaptic depolarization. *J Physiol (Lond)* 456:453–471.
- Wang H, Kunkel DD, Schwartzkroin PA, Tempel BL (1994) Localization of Kv1.1 and Kv1.2, two K channel proteins, to synaptic terminals, somata, and dendrites in the mouse brain. *J Neurosci* 14:4588–4599.
- Westerfield M, Joyner RW, Moore JW (1978) Temperature-sensitive conduction failure at axon branch points. *J Neurophysiol* 41:1–8.
- Zhou L, Zhang CL, Messing A, Chiu SY (1998) Temperature-sensitive neuromuscular transmission in Kv1.1 null mice: role of potassium channels under the myelin sheath in young nerves. *J Neurosci* 18:7200–7215.